Research Square

Preprints are preliminary reports that have not undergone peer review.
They should not be considered conclusive, used to inform clinical practice,
or referenced by the media as validated information.

Comparative morphology of the labium and external efferent system in the Janeirona clade (Hemiptera: Pentatomidae: Ochlerini)

Vinícius Gomes Sampaio

sampaiovgs@gmail.com

Universidade Federal do Rio Grande do Sul

Nathaly Lima Rodrigues

Universidade Federal do Rio Grande do Sul

Luiz Alexandre Campos

Universidade Federal do Rio Grande do Sul

Research Article

Keywords:

Posted Date: November 9th, 2026

DOI: https://doi.org/10.21203/rs.3.rs-10594021/v1

License: This work is licensed under a Creative Commons Attribution 4.0 International License.
Read Full License

Additional Declarations: No competing interests reported.

Comparative morphology of the labium and external efferent system in the *Janeirona* clade (Hemiptera: Pentatomidae: Ochlerini)

Vinícius Gomes Sampaio, Nathaly Lima Rodrigues and Luiz Alexandre Campos*

Universidade Federal do Rio Grande do Sul, Instituto de Biociências, Departamento de Zoologia, Av. Bento Gonçalves 9500, 91501-970 Porto Alegre, RS, Brazil.

*Corresponding author: sampaiovgs@gmail.com

Orcid:

VGS: https://orcid.org/0000-0002-1392-8444

NLR: https://orcid.org/0009-0007-3081-4792

LAC: https://orcid.org/0000-0001-5414-8746

Acknowledgements. We are thankful to CAPES (VGS) and CNPq [308556/2022-4] (LAC) for the scholarships.

Abstract. The labium and the external scent efferent system (ESES) are important characters in Heteroptera systematics. This study provides a comparative morphological analysis of these structures in genera within the Janeirona clade of Ochlerini (Pentatomidae: Discocephalinae), characterized by a subdivision in labiomere II. Using light and scanning electron microscopy (SEM), 15 species were investigated, including five outgroups. Results confirm that the subdivision in labiomere II is a functional intercalary segment, exhibiting articulation and intrinsic musculature. Two distinct morphological types of intercalary segments were identified: a dilated type with a wide range of motion, and a flat, short and less mobile type. Regarding the ESES, the clade shares an elliptical, ventrolaterally oriented ostiole and a spout-shaped peritreme. Detailed SEM imaging further revealed specialized scale-like microsculptures on the peritremal surface and complex spiracular filter systems. These findings provide the first high-resolution characterization of the labial intercalary segment and significantly expand the morphological data available for the tribe Ochlerini. This study offers relevant insights for future taxonomic and phylogenetic research aimed at refining the classification of Pentatomidae.

Introduction

The suborder Heteroptera is distinguished from other insect groups by the combination of the external scent efferent system (ESES), and the labium forming an elongated, segmented tube (Grazia et al. 2015; Schuh and Weirauch 2020). The labium is highly conserved within the Heteroptera infraorders, varying mostly in the number of segments (labiomeres); most families have four labiomeres, but three are seen in Reduviidae (Weirauch 2008). In contrast, the ESES morphology is highly variable between and within groups of Heteroptera, being useful for delimiting characters for phylogenetic inference and for taxonomic identification in different levels (Kment and Vilímová 2010; Barão et al. 2017; Weiler et al. 2017; Schuh and Weirauch 2020; Genevcius et al. 2021).

The ESES plays an important role in the chemical communication of true bugs, being indispensable for their defense against predators. The system is composed by paired metathoracic scent glands, in the adults, which release repellent secretions (allomones) through specialized cuticular structures such as the ostiole, peritreme and the evaporatorium. The ostiole is the opening for the draining of the secretions of metathoracic scent glands; the peritreme consists of a cuticular expansion or excavation adjacent to the ostiole of the thoracic gland, responsible for conducting secretions to the evaporatorium, which is composed by cuticular mycoid microsculpture present on the meso- and metapleural surface, responsible for spreading and containing the secretion in a delimited pleural area (protecting the insect of the secretion toxicity) and helping volatilization (Staddon 1979, 1986; Aldrich 1988; Kment et al. 2012; Weber et al. 2017).

Although studies of the ESES microsculpture under scanning electron microscopy (SEM) dates from the 1960s (for a review see Kment and Vilímová 2010), it was only recently that SEM techniques began to be employed in systematized comparative studies of groups within Pentatomoidea and Pentatomidae. In the seminal work by Kment and Vilímová (2010) the ESES in Pentatomoidea was characterized in detail, and standardized terminology was proposed. They distinguished six types of peritreme in the superfamily: auricle, spout, groove, ruga, disc and lobes; and highlighted the different parts composing the mushroom bodies of the evaporatorium: cap, stem, bridges, alveoli and trabeculae. This work served as a basis for studies in Pentatomidae (Carpocorini) (Barão et al. 2017), Aphylidae (Kment et al. 2012) and Scutelleridae (Weiler et al. 2017), however, the ESES fine morphology of many other groups remain unstudied.

The labium has been considered of taxonomic value in Pentatomidae, frequently used in keys and diagnoses to genera and species (e.g., Rolston and McDonald 1979; Grazia et al. 2015; Rider et al. 2018; Schuh and Weirauch 2020), being highly variable in length in most subfamilies. However, in the *Janeirona* Distant, 1911 clade (sensu Sampaio and Campos 2023) of Discocephalinae, the proximal portion of labiomere II presents what previous authors have named as “pseudo-segment" (Kormilev 1949, 1955, 1956), “pseudo-base” (Ruckes 1958), or "intercalary segment” (Rolston 1992), what suggest different interpretations of the morphology and functionality of the structure.

Discocephalinae is one of the 10 subfamilies of Pentatomidae, consisting of a Neotropical group with more than 300 species and 77 genera divided in two tribes, Discocephalini and Ochlerini (Grazia et al. 2015; Rider et al., 2018); in the latter belongs the *Janeirona* clade composed by *Adoxoplatys* Breddin, 1903, *Neoadoxoplatys* Kormilev, 1956, and *Paropsocolis* Sampaio and Campos, 2023 (Sampaio and Campos 2023). In this study we investigate the morphology of the labium and ESES of the genera in the *Janeirona* clade, following a comparative approach with species of other pentatomid genera.

Materials and Methods

A total of 15 species were studied using both light and scanning electron microscopy (SEM) (Table 1; Fig. 1): nine species of the four genera of the *Janeirona* clade, *Placocoris viridis* Mayr, 1864, *Macropygium reticulare* (Fabricius, 1803), *Edessa rufomarginata* (De Geer 1773), *Euschistus heros* (Fabricius 1798) and *Chinavia obstinata* (Stål 1860). The last five species lack an intercalary segment, the usual condition in Pentatomidae, and were included in the study as a proxy from which the labium of the species in the *Janeirona* clade is described. The ESES of all 14 species are described following Barão et al. (2017).

The specimens examined belong to the following collections: AMNH: American Museum of Natural History, New York, USA; CEIOC: Coleção Entomológica, Instituto Oswaldo Cruz, Rio de Janeiro, Brazil; MNRJ: Museu Nacional do Rio de Janeiro, Rio de Janeiro, Brazil; MRCN: Museu de Ciências Naturais do Rio Grande do Sul, Porto Alegre, Brazil; MZSP: Museu de Zoologia da Universidade de São Paulo, São Paulo, Brazil; URFG: Coleção de Hemiptera, Universidade Federal do Rio Grande do Sul, Porto Alegre, Brazil.

Labia and pleuron were relaxed using a modified Barber's fluid mixture (Stueben and Linsenmair 2008), removed using forceps and ophthalmic scalpel, kept submerged in contact lens cleaning solution for 48 hours and then agitated in an ultrasonic bath (40 kHz) with water and detergent for 10 minutes. In sequence, the structures were dried at 50ºC for 48 hours, sputter-coated with carbon and gold and observed using a Zeiss Evo MA10 and a Zeiss MEV-FEG/FIB Auriga scanning electron microscopes. The terminology follows Kment and Vilímová (2010) for the external scent efferent system. Articulation movement of the labial intercalary segment was tested using two forceps after submersion in hot water for 5 minutes.

Table 1. Species of Pentatomidae by subfamily used in this study. ESES: external scent efferent system.

Subfamily	Species	ESES	Labium
Discocephalinae	*Adoxoplatys comis* Breddin, 1903	X	X
	Adoxoplatys brasiliensis Kormilev, 1951	X	X
	Adoxoplatys gallardoi Kormilev, 1951		X
	Janeirona insignis Distant, 1911	X	X
	Janeirona bergi (Kormilev, 1956)	X	X
	Janeirona costalimai (Pirán, 1962)		X
	Janeirona flavipes Sampaio and Campos, 2024		X
	Janeirona stenosa Sampaio and Campos, 2024	X	
	Neoadoxoplatys longirostra Ruckes, 1958		X
	Macropygium reticulare (Fabricius, 1803)	X	X
	Paropsocolis convergens Sampaio and Campos, 2023	X	X
	Placocoris viridis Mayr, 1864	X	X
Edessinae	*Edessa rufomarginata* (De Geer, 1773)	X	X
Pentatominae	*Chinavia obstinata* (Stål, 1860)	X	X
	Euschistus heros (Fabricius, 1798)	X	X

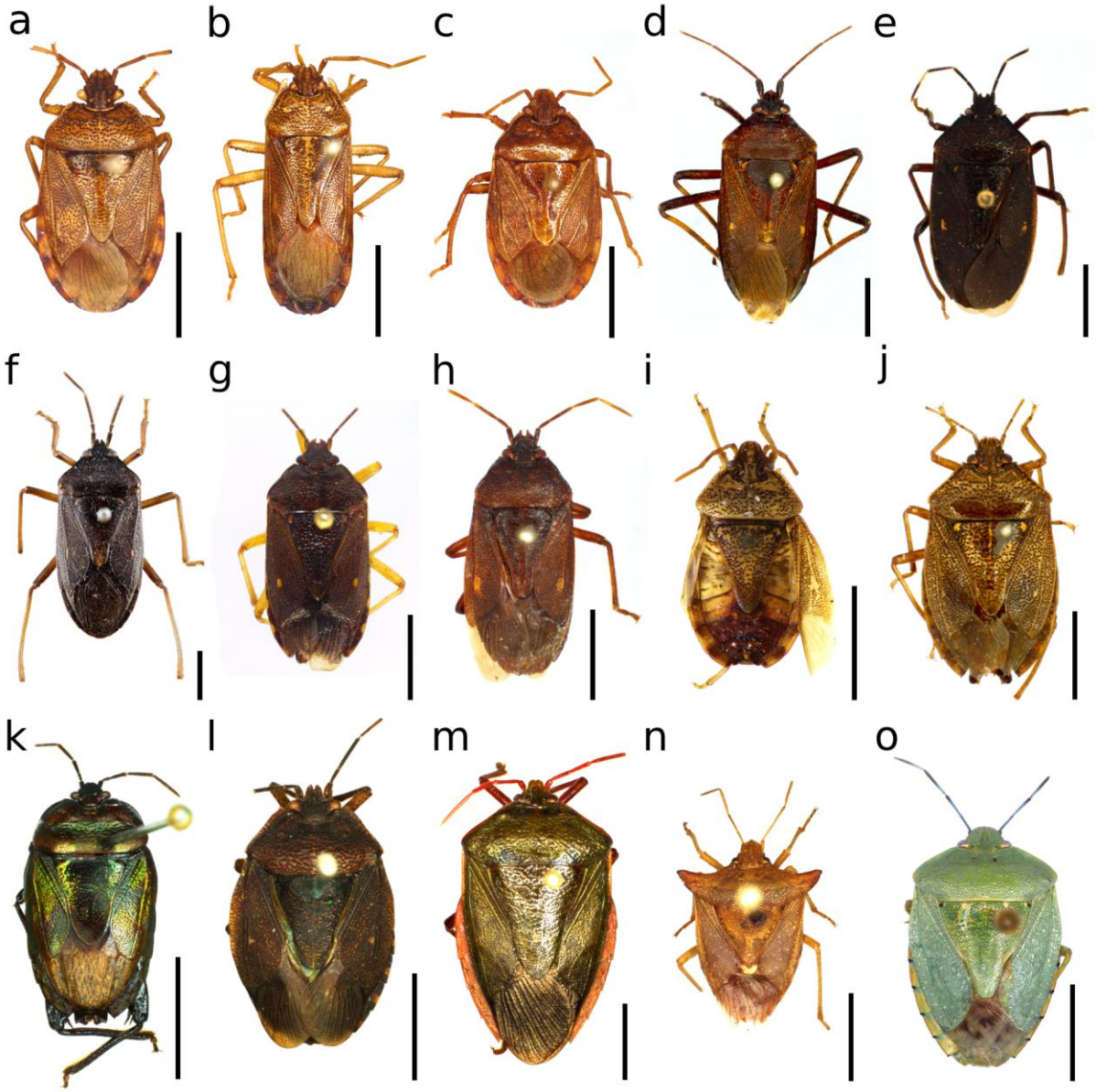


Fig. 1 Dorsal habitus of the studied species. **a** *Adoxoplatys comis* Breddin, 1903; **b** *Adoxoplatys brasiliensis* Kormilev, 1951; **c** *Adoxoplatys gallardoi* Kormilev, 1951; **d** *Neoadoxoplatys longirostra* Ruckes, 1958; **e** *Janeirona insignis* Distant, 1911; **f** *Janeirona bergi* (Kormilev, 1956); **g** *Janeirona costalimai* (Pirán, 1962); **h** *Janeirona flavipes* Sampaio and Campos, 2024; i *Janeirona stenosa* Sampaio and Campos, 2024; **j** *Paropsocolis convergens* Sampaio and Campos, 2023; **k** *Placocoris viridis* Mayr, 1864; **l** *Macropygium reticulare* (Fabricius, 1803); **m** *Edessa rufomarginata* (De Geer, 1773); **n** *Euschistus heros* (Fabricius, 1798); **o** *Chinavia obstinata* (Stål, 1860). Scale bars = 5 mm.

Results

Labium

This section focuses on the proximal portion of the labiomere II, henceafter termed intercalary segment, observed in all the *Janeirona* clade. Because we successfully simulated articulation movements between the labiomere II (Fig. 2, a) and the intercalary segment (Fig. 2, b), we chose the latter terminology instead of "pseudo-segment" or "pseudo-base".

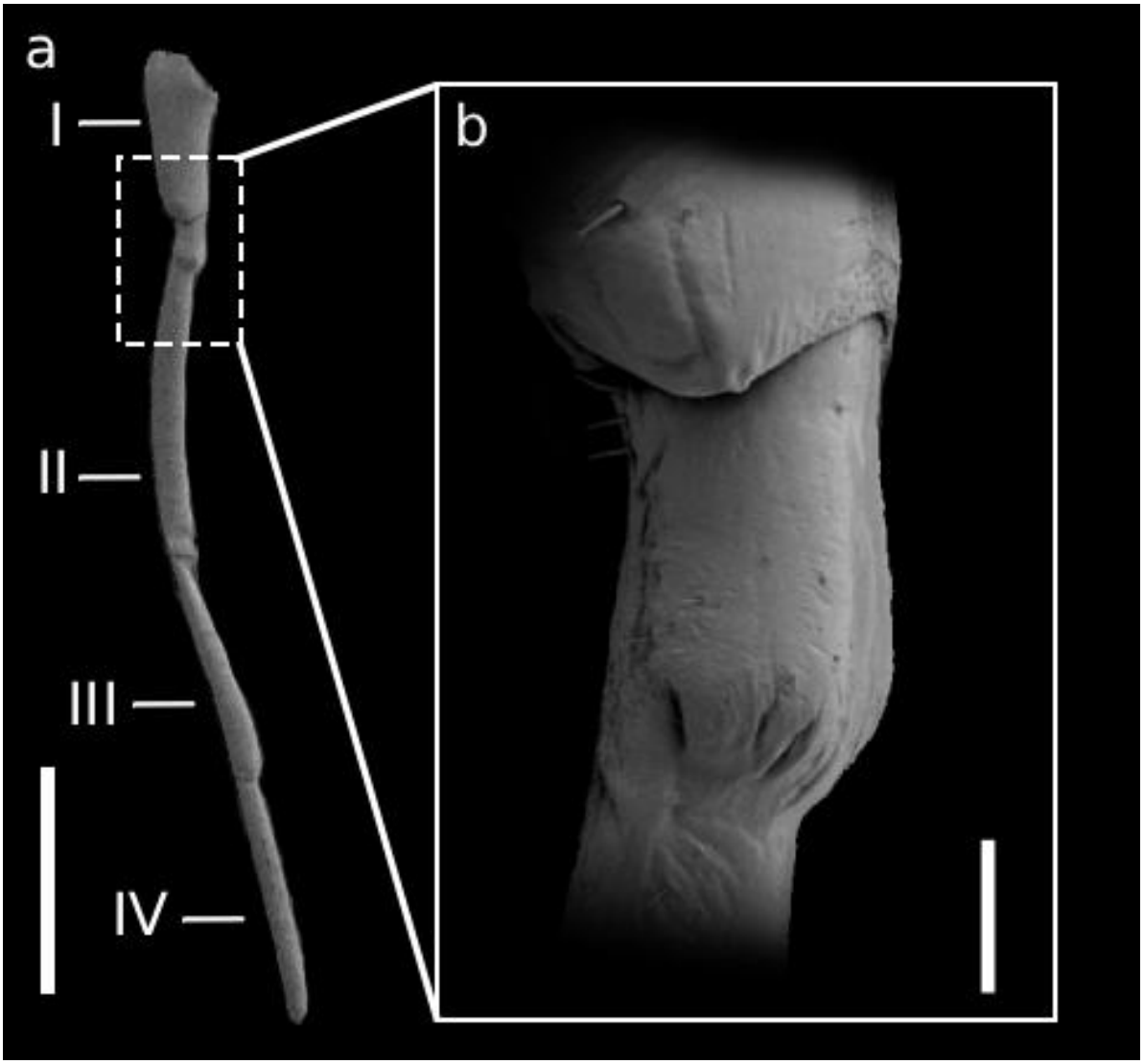


Fig. 2 Labium of *Adoxoplatys brasiliensis* Kormilev, 1951, with the detail of intercalary segment. Scale bars: **a** = 1 mm, **b** = 100 μm.

We were also able to identify intrinsic musculature and apodemes in the intercalary segment (Fig. 3), although it was not possible to discern specific muscles and their insertion points inside the intercalary segment or the other labial segments.

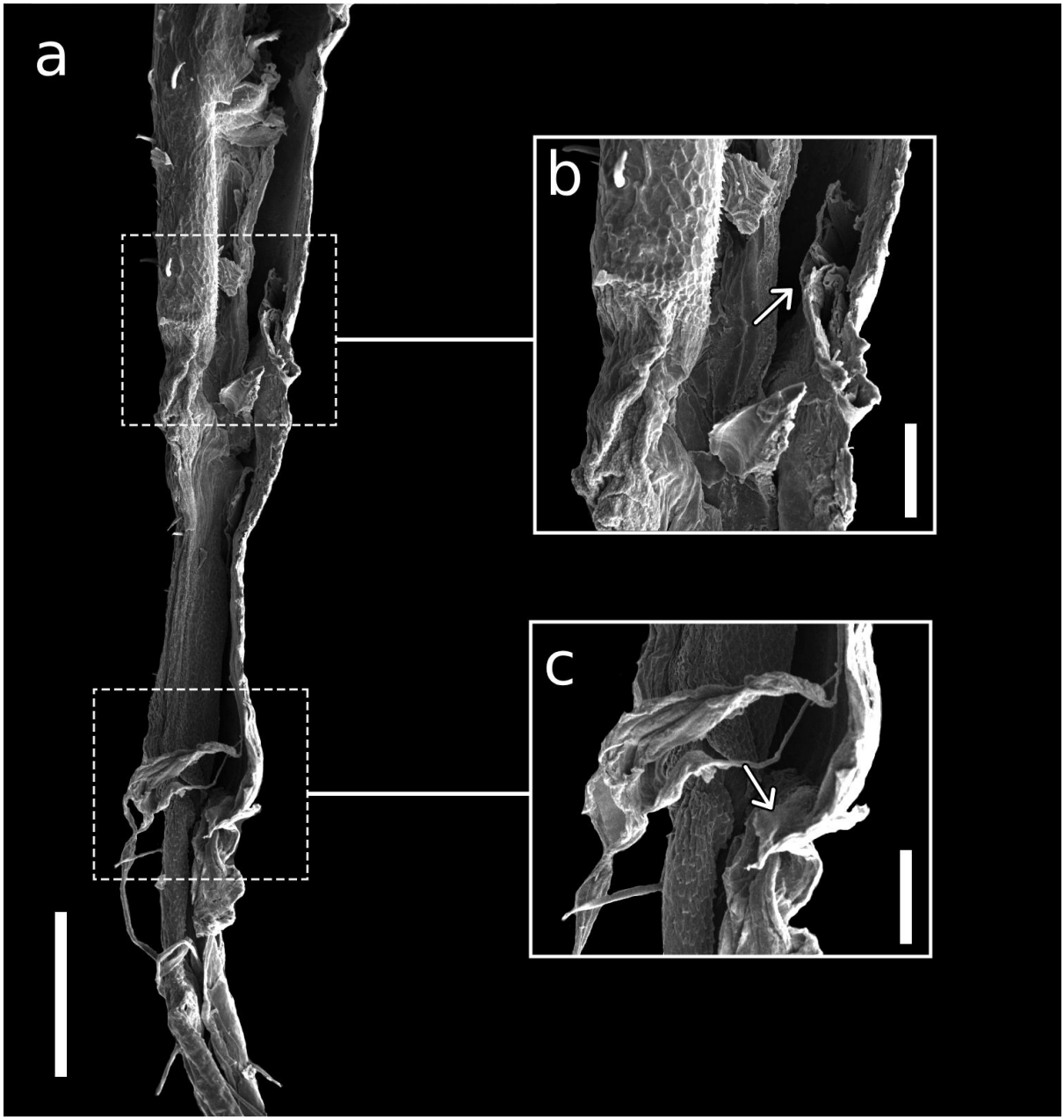


Fig. 3 Longitudinal section of intercalary segment of *Adoxoplatys comis* Breddin, 1903. Arrows indicates apodemes. Scale bars: **a** = 200 µm, **b** = 50 µm, **c** = 50 µm.

Species in the *Janeirona* clade

Adoxoplatys comis Breddin, 1903 (Figs 1a, 4a)

Intercalary segment constricted in the anteromedian portion, measuring approximately 1/5 of labiomere II; ventroproximal surface with a row of three sensillae on each side; dorsal surface strongly dilated in distal portion.

Adoxoplatys brasiliensis Kormilev, 1951 (Figs 1b, 2, 4b)

Intercalary segment not constricted, measuring approximately 1/7 of labiomere II; ventroproximal surface with a row of three sensillae on each side; dorsal surface strongly dilated in distal portion.

Adoxoplatys gallardoi Kormilev, 1951 (Figs 1c, 4c)

Intercalary segment slightly constricted in the anteromedian portion, measuring approximately 1/6 of labiomere II and wider than its proximal portion; ventroproximal surface with a row of three sensillae on each side; dorsal surface strongly dilated in distal portion; laterodistal surface with a sensilla.

Neoadoxoplatys longirostra Ruckes, 1958 (Figs 1d, 4d)

Intercalary segment slightly constricted in the anteromedian portion, measuring approximately 1/5 of labiomere II and wider than its proximal portion; ventroproximal surface slightly projected as flaps, with a row of three sensillae on each side; ventrodistal surface with scale-like microsculptures; dorsal surface surface strongly dilated; laterodistal surface with one long sensilla.



Fig. 4 Comparison of intercalary segments of **a** *Adoxoplatys comis* Breddin, 1903; **b** *Adoxoplatys brasiliensis* Kormilev, 1951; **c** *Adoxoplatys gallardoi* Kormilev, 1951; **d** *Neoadoxoplatys longirostra* Ruckes, 1958. Scale bars = 100 µm.

Janeirona insignis Distant, 1911 (Figs 1e, 5a)

Intercalary segment not constricted, measuring approximately 1/10 of labiomere II and as wide as its proximal portion; ventroproximal surface slightly projected as flaps, with a row of three sensillae on each side; ventrodistal surface with scale-like microsculptures; dorsal surface not dilated; laterodistal surface with three long sensilla.

Janeirona bergi (Kormilev, 1956) (Figs 1f, 5b)

Intercalary segment not constricted, measuring approximately 1/8 of labiomere II and as wide as its proximal portion; ventroproximal surface slightly projected as flaps, with a row of three sensillae on each side; ventrodistal surface with scale-like microsculptures; dorsal surface not dilated; laterodistal surface with three long sensilla.

Janeirona costalimai (Pirán, 1962) (Figs 1g, 5c)

Intercalary segment not constricted, measuring approximately 1/5 of labiomere II and slightly wider than its proximal portion; ventroproximal surface slightly projected as flaps, with a row of three sensillae on each side; ventrodistal surface with scale-like microsculptures; dorsal surface not dilated; laterodistal surface with one long sensilla.

Janeirona flavipes Sampaio and Campos, 2024 (Figs 1h, 5d)

Intercalary segment not constricted, measuring approximately 1/7 of labiomere II and slightly wider than its proximal portionwider than it; ventroproximal surface slightly projected as flaps, with a row of three sensillae on each side; ventrodistal surface with a scale-like microsculptures; dorsal surface not dilated; laterodistal surface with one sensilla.

Paropsocolis convergens Sampaio and Campos, 2023 (Figs 1j, 5e)

Intercalary segment not constricted, measuring approximately 1/10 of labiomere II and as wide as its proximal portion; ventroproximal surface slightly projected as flaps, with a row of three sensillae on each side; ventrodistal surface with scale-like microsculptures; dorsal surface not dilated; laterodistal surface with minute sensillae.



Fig. 5 Comparison of intercalary segments of **a** *Janeirona insignis* Distant, 1911; **b** *Janeirona bergi* (Kormilev, 1956); **c** *Janeirona costalimai* (Pirán, 1962); **d** *Janeirona flavipes* Sampaio and Campos, 2024; **e** *Paropsocolis convergens* Sampaio and Campos, 2023. Scale bars = 100 µm.

Species outside the *Janeirona* clade

In all the other species studied (Fig. 6) the labiomere II is not subdivided by a surrounding suture. In *P. viridi*s (Fig. 6a), *M. reticulare* (Fig. 6b) and *E. rufomarginata* (Fig. 6c) there is no discernible delimitation at all, but *E. heros* (Fig. 6d) and *C. obstinata* (Fig. 6e) have a shallow impression on the lateral and dorsal surfaces, although it does not surround the labium and lacks a membranous ventral surface. We failed to simulate articulation movement in the proximal portion of labiomere II in any of these species, unlike in species of the *Janeirona* clade.

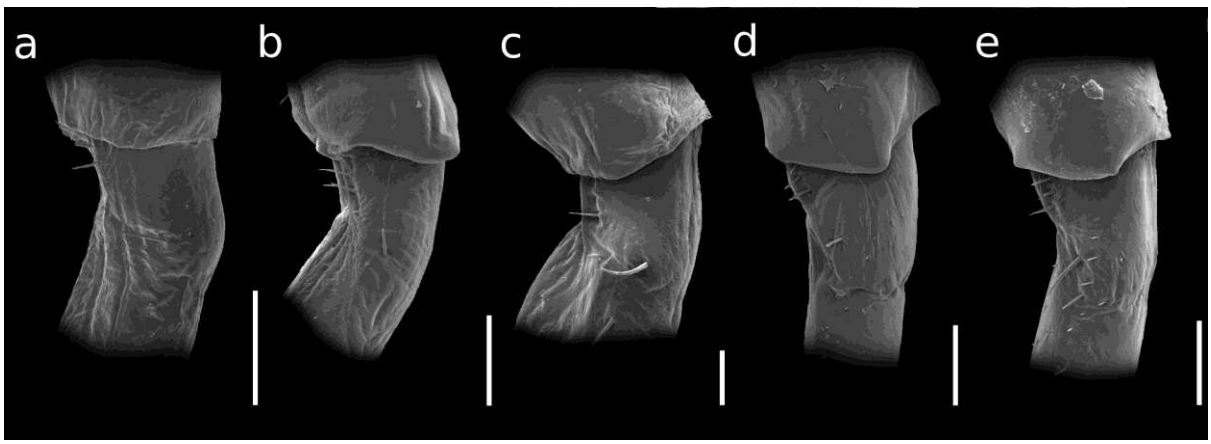


Fig. 6 Comparison of intercalary segments of **a** *Placocoris viridis* Mayr, 1864; **b** *Macropygium reticulare* (Fabricius, 1803); **c** *Edessa rufomarginata* (De Geer, 1773); **d** *Euschistus heros* (Fabricius, 1798); **e** *Chinavia obstinata* (Stål, 1860). Scale bars = 100 µm.

ESES

Species in the *Janeirona* clade (Fig. 7)

All species within the *Janeirona* clade share the following general ESES morphology. Ostiole elliptical, oriented ventrolaterally, visible in lateral view, and placed closer to the metacoxal cavity than to the lateral margin of metapleuron. Peritreme spout-shaped. Evaporatorium well-developed on meso- and metapleuron; on metapleuron, extending from the area between the coxal cavities to the last third of the ostiolar plate; on mesopleuron, covering part of the mesepimeron along the spiracular margin to the lateral pleural margin; evaporatorium with several minute sensillae; mushroom bodies irregular, alveoli with several trabeculae. Metathoracic spiracle with filter system processes of irregular diameter and connected to each other by lateral expansions.

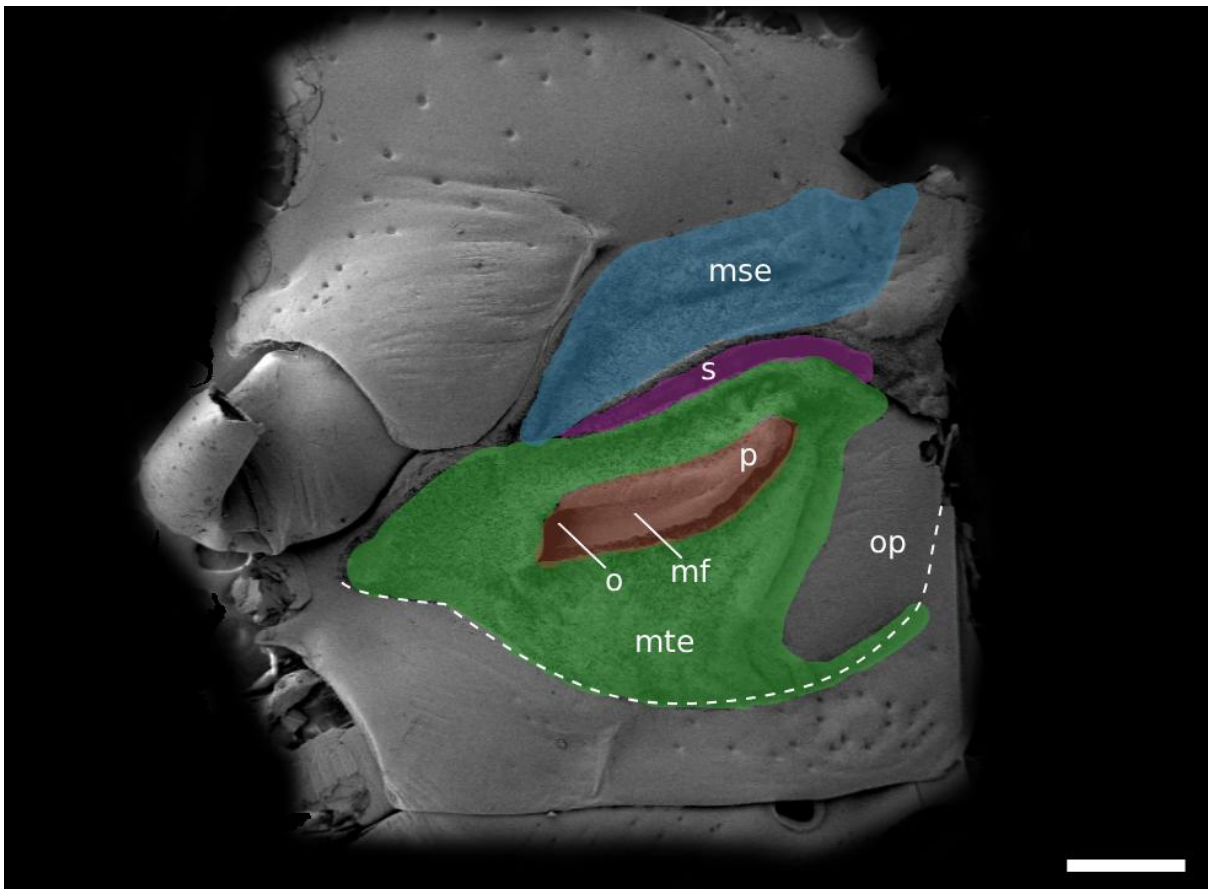


Fig. 7 External scent efferent system map over the meso- and metapleuron of *Janeirona insignis* Distant, 1911. Abbreviations: mf = peritremal median furrow; mse = mesopleural evaporatorium (blue shaded); mte = metapleural evaporatorium (green shaded); o = ostiole; op = ostiolar plate (dashed line); p = peritreme (orange shaded); s = spiracular filter system (pink shaded). Scale bar = 500 μm.

Adoxoplatys comis Breddin, 1903 (Figs 1a, 8)

Peritreme directed laterally; lateral margin round, elevated and parallel to the surrounding pleuron; median furrow developed basally (Fig. 8b); peritremal surface covered with scale-like microsculptures and sparse sensillae (Fig. 8c). Metapleural evaporatorium with posterior and lateral margins elevated, lateral margin convex. Metathoracic spiracle wide; filter system processes of irregular diameter and connected to each other by lateral expansions, space between processes subequal to the width of one process (Fig. 8e).

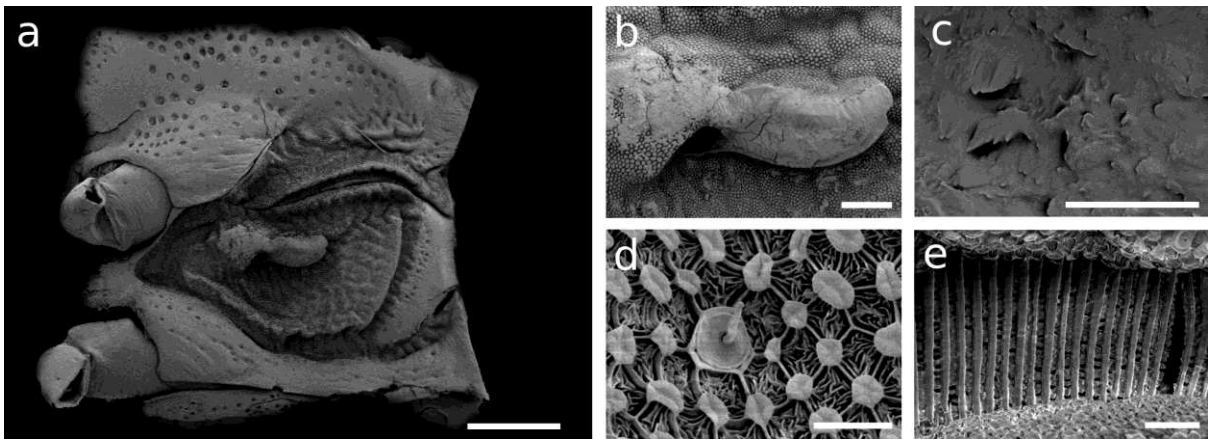


Fig. 8 External scent efferent system of *Adoxoplatys comis* Breddin, 1903. **a** meso- and metapleuron; **b** peritreme; **c** peritremal surface; **d** detail of evaporatorium; **e** spiracular filter system. Scale bars: **a** = 500 µm, **b** = 100 µm, **c**, **d** = 10 µm, **e** = 20 µm.

Adoxoplatys brasiliensis Kormilev, 1951 (Figs 1b, 9)

Peritreme directed laterally; lateral margin round, elevated and parallel to the surrounding pleuron; anterior margin slightly folded backwards; median furrow well-developed (Fig. 9b); peritremal surface covered with scale-like microsculptures (Fig. 9c). Metapleural evaporatorium with posterior and lateral margins elevated, lateral margin convex. Metathoracic spiracle narrow; filter system processes of irregular diameter and connected to each other by lateral expansions, space between processes subequal to the width of one process (Fig. 9e).

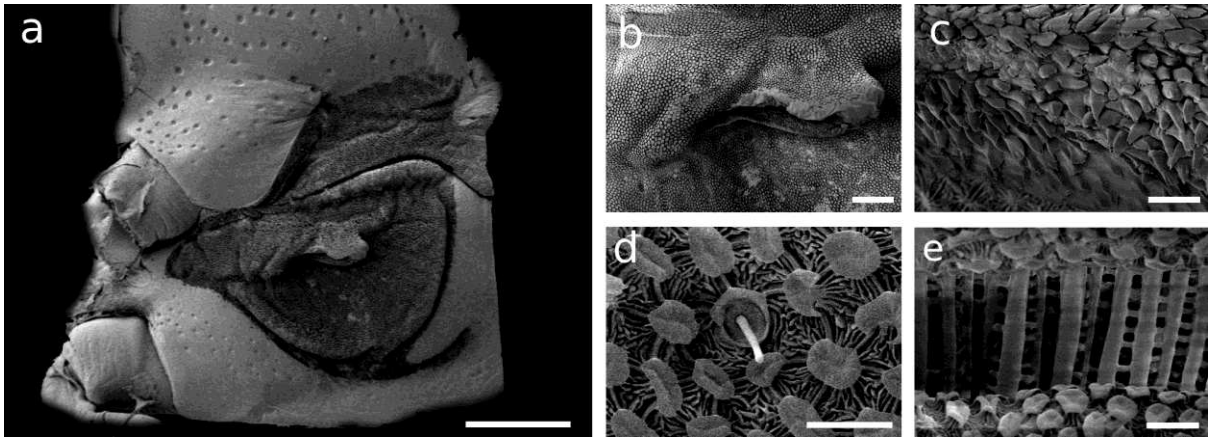


Fig. 9 External scent efferent system of *Adoxoplatys brasiliensis* Kormilev, 1951. **a** meso- and metapleuron; **b** peritreme; **c** peritremal surface; **d** detail of evaporatorium; **e** spiracular filter system. Scale bars: **a** = 500 µm, **b** = 100 µm, **c**–**e** = 10 µm.

Janeirona insignis Distant, 1911 (Figs 1e, 7, 10)

Peritreme directed anterolaterally, tapering towards its apex, elevated and parallel to the surrounding pleuron ; median furrow well-developed (Fig. 10b); peritremal surface covered by scale-like microsculptures with serrate margins (Fig. 10c). Metapleural evaporatorium with lateral margin elevated, sinuous. Metathoracic spiracle wide; filter system processes of irregular diameter and connected to each other by lateral expansions, space between processes approximately twice the width of one process (Fig. 10e).

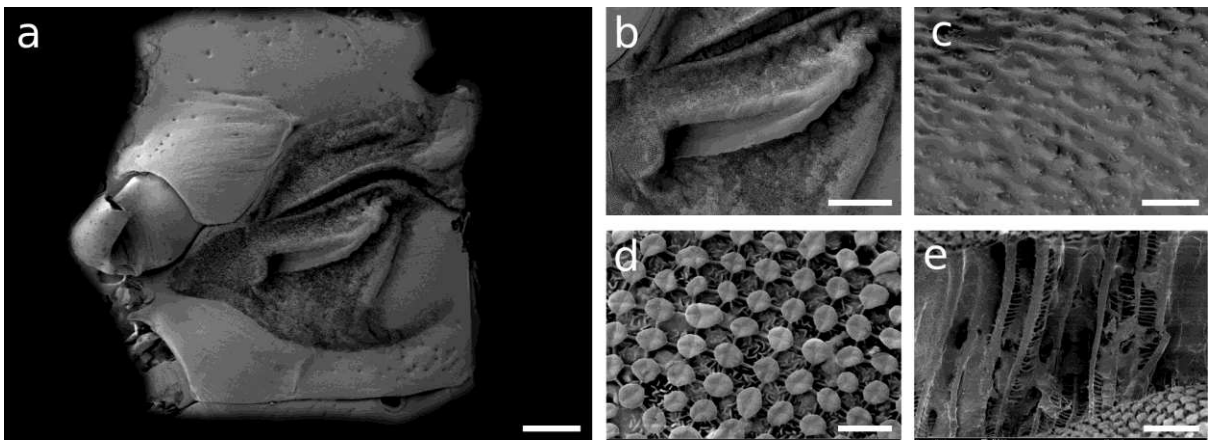


Fig. 10 External scent efferent system of *Janeirona insignis* Distant, 1911. **a** meso- and metapleuron; **b** peritreme; **c** peritremal surface; **d** detail of evaporatorium; **e** spiracular filter system. Scale bars: **a** = 500 µm, **b** = 300 µm, **c**, **d** = 10 µm, **e** = 20 µm.

Janeirona bergi (Kormilev, 1956) (Figs 1f, 11)

Peritreme directed anterolaterally, tapering towards its apex, elevated and parallel to the surrounding pleuron; median furrow well-developed (Fig. 11b); peritremal surface covered by scale-like microsculptures with serrate margins (Fig. 11c). Metapleural evaporatorium with posterior and lateral margins slightly elevated, lateral margin slightly convex. Metathoracic spiracle wide; filter system processes of irregular diameter and connected to each other by lateral expansions, space between processes approximately twice the width of one process (Fig. 11e).

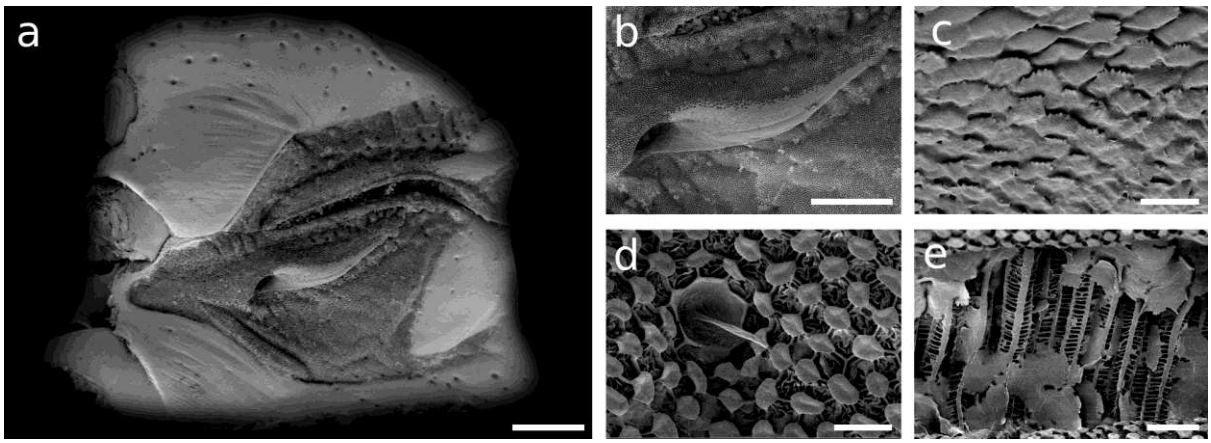


Fig. 11 External scent efferent system of *Janeirona bergi* (Kormilev, 1956). **a** meso- and metapleuron; **b** peritreme; **c** peritremal surface; **d** detail of evaporatorium; **e** spiracular filter system. Scale bars: **a** = 500 µm, **b** = 300 µm, **c**, **b** = 10 µm, **e** = 20 µm.

Janeirona stenosa Sampaio and Campos, 2024 (Figs 1i, 12)

Peritreme directed anterolaterally, tapering towards its apex, elevated and parallel to the surrounding pleuron; median furrow well-developed (Fig. 12b); peritremal surface covered by scale-like microsculptures with serrate margins (Fig. 12c). Metapleural evaporatorium with posterior and lateral margins elevated, lateral margin sinuous. Metathoracic spiracle wide; filter system processes of irregular diameter and connected to each other by lateral expansions, space between processes approximately twice the width of one process (Fig.12e).

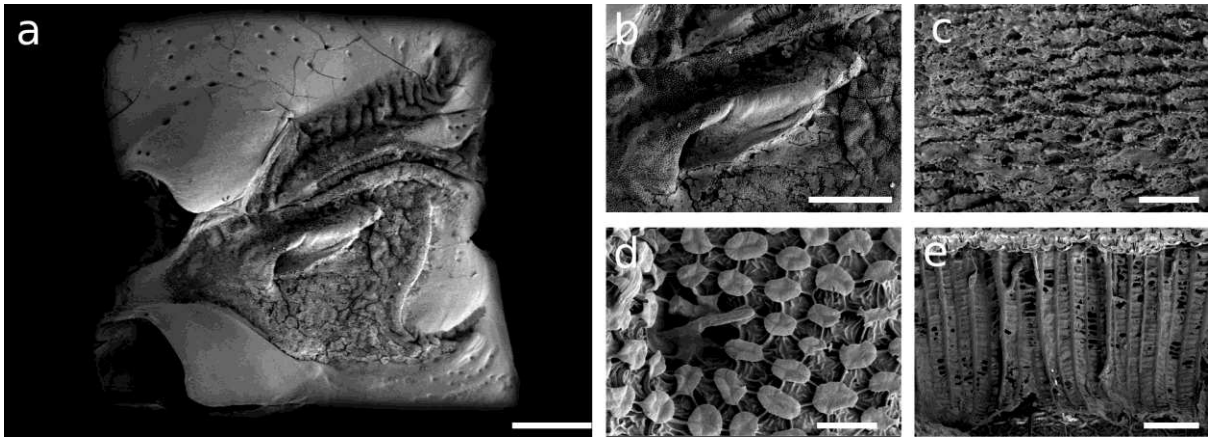


Fig. 12 External scent efferent system of *Janeirona stenosa* Sampaio and Campos, 2024. **a** meso- and metapleuron; **b** peritreme; **c** peritremal surface; **d** detail of evaporatorium; **e** spiracular filter system. Scale bars: **a** = 500 µm, **b** = 300 µm, **c, d** = 10 µm, **e** = 20 µm.

Paropsocolis convergens Sampaio and Campos, 2023 (Figs 1j, 13)

Peritreme directed anterolaterally, tapering towards its apex, elevated and parallel to the surrounding pleuron (Fig. 13b); median furrow poorly developed; peritremal surface covered by scale-like microsculptures with serrate margins (Fig. 13c). Metapleural evaporatorium with posterior and lateral margins elevated, lateral margin subrectilinear. Metathoracic spiracle wide; filter system processes of irregular diameter and connected to each other by lateral expansions, space between processes aproximately twice the width of one process (Fig. 13e).

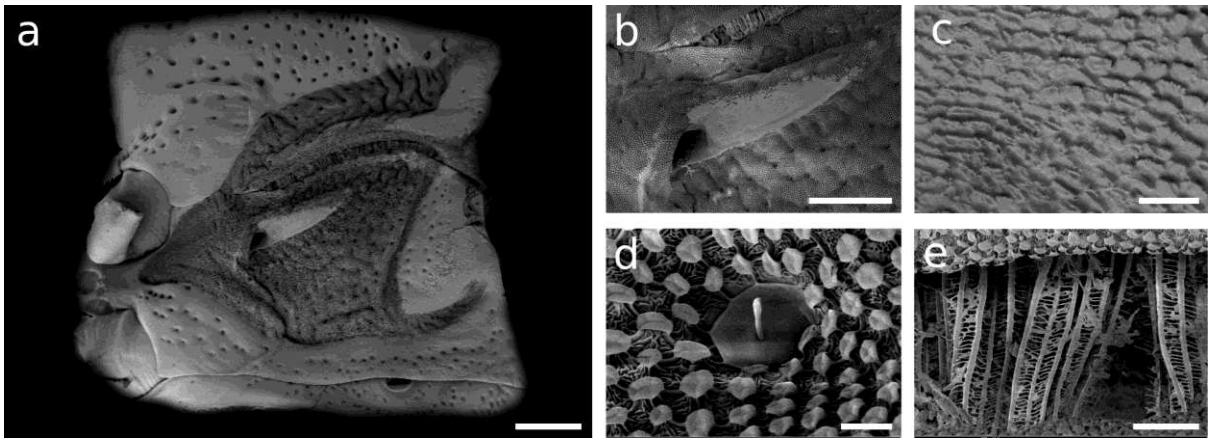


Fig. 13 External scent efferent system of *Paropsocolis convergens* Sampaio and Campos, 2023. **a** meso- and metapleuron; **b** peritreme; **c** peritremal surface; **d** detail of evaporatorium; **e** spiracular filter system. Scale bars: **a** = 500 µm, **b** = 300 µm, **c, d** = 10 µm, **e** = 30 µm.

Species outside the *Janeirona* clade

All species outside the *Janeirona* clade share the following general ESES morphology. Ostiole elliptical, oriented ventrolaterally, visible in lateral view. Evaporatorium well-developed on meso- and metapleuron; on mesopleuron, covering part of the mesepimeron along the spiracular margin to the lateral margin of the mesopleuron; evaporatorium with several sensillae; mushroom bodies irregular, alveoli with several trabeculae.

Placocoris viridis Mayr, 1864 (Figs 1k, 14)

Ostiole closer to the lateral margin of metapleuron than to the metacoxal cavity (Fig. 14a). Peritreme spout-shaped, directed laterally, elevated and parallel to the surrounding pleuron; median furrow poorly developed (Fig. 14b); peritremal surface with sparse sensillae, and covered by scale-like microsculptures (Fig. 14c). Evaporatorium, on metapleuron, extending from the area adjacent to the mesocoxal cavities to the last third of the ostiolar plate, not covering the postero-mesial part of the ostiolar plate; posterior margin concave, lateral margin slightly elevated and convex (Fig. 13a); mushroom bodies irregular, alveoli with several trabeculae (Fig. 14d). Metathoracic spiracle narrow; metapleural margin of spiracle with several sensillae; filter system processes of irregular diameter and connected to each other by lateral expansions, space between processes approximately twice the width of one process (Fig. 14e).

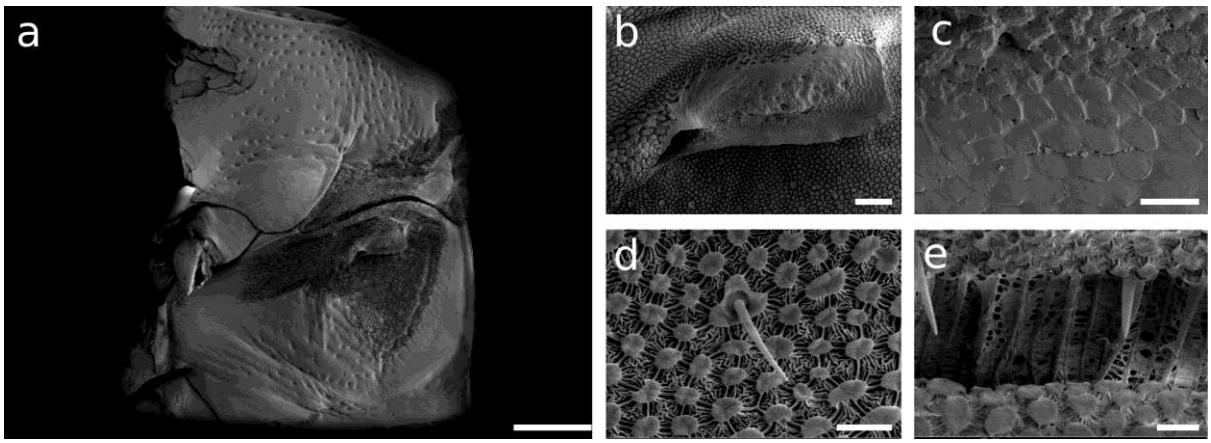


Fig. 14 External scent efferent system of *Placocoris viridis* Mayr, 1864. **a** meso- and metapleuron; **b** peritreme; **c** peritremal surface; **e** detail of evaporatoriu; **e** spiracular filter system. Scale bars: **a** = 500 µm, **b** = 100 µm, **c-e** = 10 µm.

Macropygium reticulare (Fabricius, 1803) (Figs 1l, 15)

Ostiole closer to the metacoxal cavity than to the lateral margin of metapleuron (Fig. 15a). Peritreme spout-shaped, directed laterally, lateral margin round, elevated and parallel to the surrounding pleuron; median furrow poorly

developed (Fig. 15b); peritremal surface with wrinkled microsculpture (Fig. 15c). Evaporatorium, on metapleuron, extending from the area adjacent to the coxal cavities to half of the ostiolar plate, lateral margin slightly elevated, subrectilinear (Fig. 15a). Metathoracic spiracle narrow; filter system processes of irregular diameter, surface with numerous large, spine-like projections, some merging and connecting the processes to each other, space between processes 1.5 times to twice the width of one process (Fig. 15e).

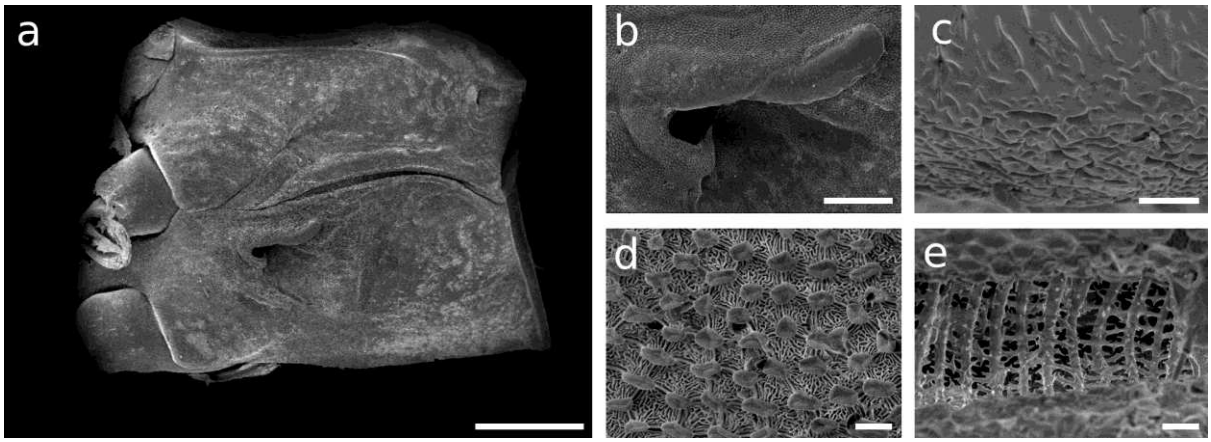


Fig. 15 External scent efferent system of *Macropygium reticulare* (Fabricius, 1803). **a** meso- and metapleuron; **b** peritreme; **c** peritremal surface; **d** detail of evaporatoriu; **e** spiracular filter system. Scale bars: **a** = 1 mm, **b** = 200 μm, **c-e** = 10 μm.

Edessa rufomarginata (De Geer, 1773) (Figs 1m, 16)

Ostiole closer to the metacoxal cavity than to the lateral margin of metapleuron (Fig. 16a). Peritreme ruga-shaped, directed anterolaterally, tapering towards its apex, elevated and parallel to the surrounding pleuron; median furrow poorly developed (Fig. 16b); peritremal surface smooth (Fig. 16c). Evaporatorium, on metapleuron, extending from the area between the coxal cavities to the last third of the ostiolar plate, posterior and lateral margins slightly elevated, lateral margin concave (Fig. 16a). Metathoracic spiracle narrow; filter system processes of irregular diameter and connected to each other by lateral expansions, space between processes approximately twice the width of one process (Fig. 16e).

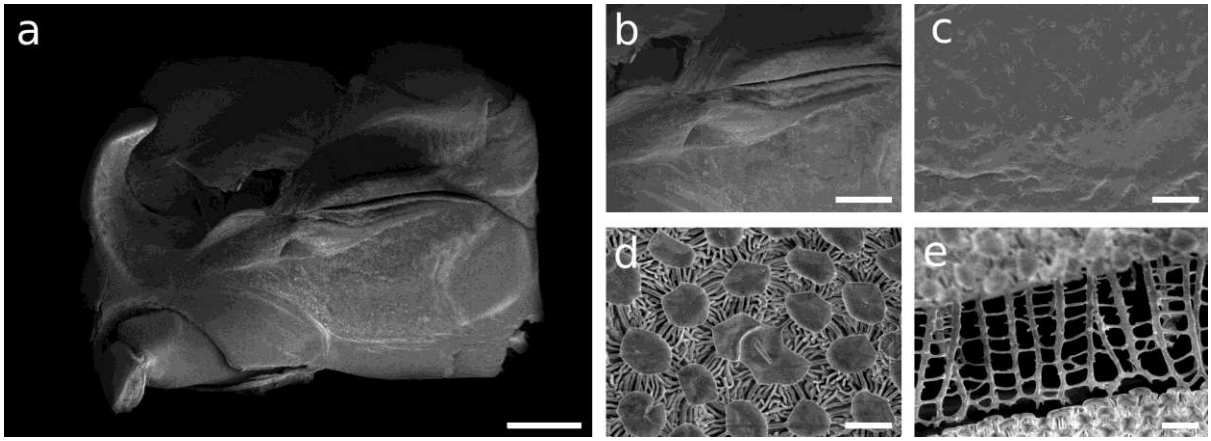


Fig. 16 External scent efferent system of *Edessa rufomarginata* (De Geer, 1773). **a** meso- and metapleuron, **b** peritreme; **c** peritremal surface; **d** detail of evaporatorium; **e** spiracular filter system. Scale bars: **a** = 1 mm, **b** = 200 µm, **c-e** = 10 µm.

Euschistus heros (Fabricius, 1798) (Figs 1n, 17)

Ostiole closer to the metacoxal cavity than to the lateral margin of metapleuron (Fig. 17a). Peritreme very reduced, spout-shaped, directed laterally, lateral margin round, elevated and parallel to the surrounding pleuron; median furrow well-developed (Fig. 17b); peritremal surface slightly wrinkled (Fig. 17c). Evaporatorium well-developed on meso- and metapleuron; on metapleuron, extending from the area between the coxal cavities to the last third of the ostiolar plate, posterior and lateral margins slightly elevated, lateral margin slightly sinuous (Fig. 17a). Metathoracic spiracle narrow; filter system processes of irregular diameter, not connected to each other; surface with numerous spine-like projections, space between processes at least twice the width of one process (Fig. 17e).

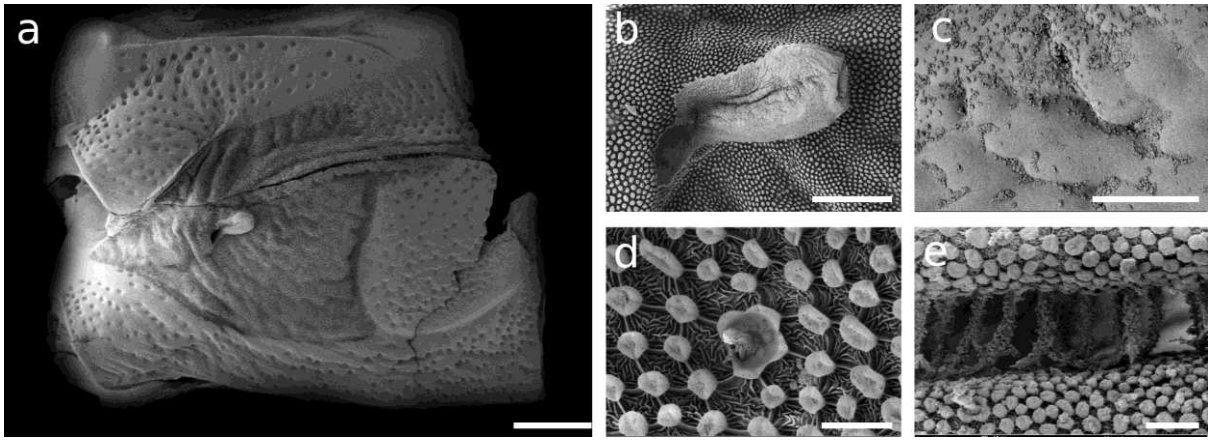


Fig. 17 External scent efferent system of *Euschistus heros* (Fabricius, 1798). **a** meso- and metapleuron; **b** peritreme; **c** peritremal surface; **d** detail of evaporatorium; **e** spiracular filter system. Scale bars: **a** = 500 µm, **b** = 100 µm, **c**, **d** = 10 µm, **e** = 20 µm.

Chinavia obstinata (Stål, 1860) (Figs 1o, 18)

Ostiole closer to the metacoxal cavity than to the lateral margin of metapleuron (Fig. 18a). Peritreme ruga-shaped, directed anterolaterally, tapering towards its apex, parallel to the surrounding pleuron; median furrow well-developed (Fig. 18b); peritremal surface covered with scale-like microsculptures with marginal spine-like protuberances (Fig. 18c). Evaporatorium well-developed on meso- and metapleuron; on metapleuron, extending from the area between the coxal cavities to the last third of the ostiolar plate, posterior and lateral margins not elevated, lateral margin concave (Fig. 18d). Metathoracic spiracle narrow; filter system processes of irregular diameter; surface with numerous spine-like projections, some merging and connecting the processes to each other, space between processes approximately twice the width of one process (Fig. 18e).

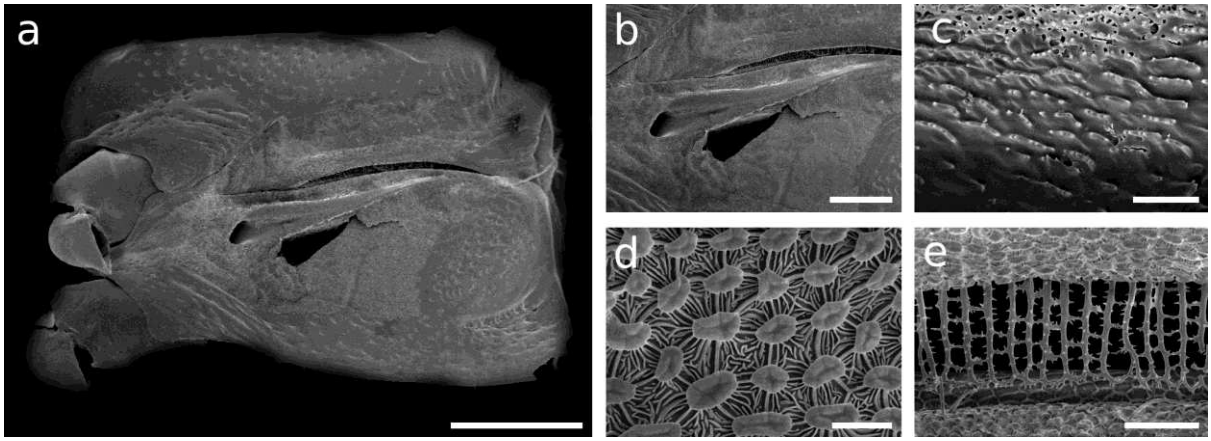


Fig. 18 External scent efferent system of *Chinavia obstinata* (Stål, 1860). **a** meso- and metapleuron; **b** peritreme; **c** peritremal surface; **d** detail of evaporatorium; **e** spiracular filter system. Scale bars: **a** = 1 mm, **b** = 100 μm, **c**, **d** = 10 μm, **e** = 20 μm.

Discussion

Labium

Arthropod mouthparts share developmental processes and controlling genes, a conserved feature in insect evolution. Despite the underlying shared mechanisms, there is a strong tendency for morphological diversification of the different mouthparts within restricted groups as a consequence of adaptations to lifestyle and diet, as seen in most insect orders (Angelini and Smith 2019). Such plasticity led to the evolution of the unique hemipteran segmented labium. In Heteroptera, the ancestral condition of a four-segmented labium is conserved in almost all lineages, having evolved to three-segmented only in the Reduviidae as a result of the reduction of the first segment (Weirauch 2008). The Corixoidea present a highly modified labium, shortened and triangular, without apparent

segmentation (Brozek 2014). More subtle variation is found in several lineages presenting the conserved four-segmented labium, as documented in a few Pentatomoidea. The predacious pentatomids in the subfamily Asopinae show a modified labium-head articulation that allows the rostrum to turn full forward, a feature that has been linked to predation (De Clerq 2000) along with the labium being robust, thickened (Gapud 1991). In Cydnidae the genus *Prolobodes* Amyot and Serville has an expanded second labial segment, forming a sacciform compartment where the stylets are coiled (Costa Lima 1940; Martinez 2002). The presence of an intercalary segment has not been observed, to our knowledge, in any group of ground Heteroptera other than the *Janeirona* clade.

We have identified two types of intercalary segments, both represented by the subdivision of labiomere II by a surrounding suture. The first type is found in *Neoadoxoplatys* and *Adoxoplatys*, in which the dorsal surface is strongly dilated in the distal portion, and the distal articulation is completely functional, allowing a wide angular range of motion. The second type, in *Janeirona* and *Paropsocolis*, shows a more flat, not dilated dorsal surface, and the distal articulation partially functional, allowing only a restricted angular movement. The first type is more easily discernible in steromicroscopy, and usually represented by longer intercalary segments compared to the second type. It is important to highlight that although the total length of the labium varies among species in the *Janeirona* clade, there is no correlation between the labial length and the length of the intercalary segment; the latter shows no significant variation between species within each genus (Sampaio and Campos 2023; Sampaio et al. 2024, *in press*). Additionally, we observed in the pentatomines *E. heros* and *C. obistinata* a dorsal suture at the distal portion of the base of labiomere II, though not surrounding the labiomere and thus not characterizing an articulation.

Based on the genera presenting each type of intercalary segment, and considering the phylogenies available (Roell and Campos 2019; Sampaio and Campos 2023), we hypothesize the intercalary segment arose in the ancestor of the *Janeirona* clade, then reduced in the ancestor of the clade formed by the genera *Janeirona* and *Paropsocolis*. A more complete understanding on the ontogeny, function and evolution of the intercalary segment will require behavioral, histological and developmental studies.

ESES

We found little correspondence between the ESES structure and taxonomy. Most species studied have well developed metapleural evaporatoria (reduced in the ochlerine *M. reticulare*) with elevated lateral margins (not elevated in the pentatomine *C. obstinata*). The most frequent peritreme was the spout-shaped (ruga-shaped only

in *C. obstinata*), reduced in the pentatomine *E. heros*. The filter system of the metathoracic spiracle in most species showed processes connected to each other by lateral expansions, but not connected in *E. heros*, and presenting spine-like projections in *M. reticulare*, *E. heros*, and *C. obstinata*.

The edessine *E. ruformarginata* was the non-Ochlerini species sharing more morphological features of the ESES with the *Janeirona* clade. Although a robust phylogeny of subfamilies of Pentatomidae is still lacking, morphological and molecular data indicate a possible closeness between Discocephalinae and Edessinae (Roell and Campos 2019; Roca-Cusachs et al. 2022; Genevcius 2024). Whether our results reflect an evolutionary relationship is yet to be investigated with the inclusion of more taxa under a phylogenetic framework. The same applies to the possible relationship between *Placocoris* and the *Janeirona* clade, which has been proposed by Thomas (2021) based on characters of pronotum, legs and genitalia, a hypothesis also not yet submitted to phylogenetic testing.

The scale-like microstructure present on the peritreme surface of several studied species, such as *A. brasiliensis*, *J. bergi*, and *P. convergens*, may facilitate the movement of odorous secretion from the ostiole towards the evaporatorium. A directional flux facilitation has been demonstrated in similar peritreme surfaces of the pentatomine *Palomena prasina* and *Rhaphigaster nebulosa* (Hischen et al. 2018) in a study on biomimetic materials. However, we cannot ascertain if fluid secretion would behave the same way in the species we studied, due to the differences between the shape of their scales compared to those in *P. prasina* and *R. nebulosa*.

This study expands the investigation into the fine morphology of ESES, providing novel information for the tribe Ochlerini, in addition to presenting the first characterization, via scanning electron microscopy, of the labial intercalary segment in species of the *Janeirona* clade. The data presented herein may be useful in future studies focusing on the morphology of Discocephalinae and Pentatomidae, as well as in broader taxonomic and phylogenetic studies aiming to establish a natural classification of the subfamilies in Pentatomidae.

Declarations

Ethical approval. Not applicable.

Funding. Partial financial support was received from Coordenação de Aperfeiçoamento de Pessoal de Nível Superior (CAPES) (VG Sampaio) and Conselho Nacional de Desenvolvimento Científico e Tecnológico (CNPq) (grant number 308556/2022-4 to LA Campos).

Author contributions. LA Campos and VG Sampaio equally contributed to the research design and the manuscript writing. VG Sampaio and NL Rodrigues acquired the data and built the images. NL Rodrigues helped with specimen and reference organization.

Conflicts of interest/Competing interests. The authors have no conflicts of interest to declare that are relevant to the content of this article.

References

Aldrich JR (1988) Chemical ecology of the Heteroptera. Annu Rev Entomol 33:211–238. https://doi.org/10.1146/annurev.en.33.010188.001235

Angelini DR, Smith, FW (2019) Theme and variation in the development of insect mouthparts. In: Krenn HW (ed) Insect Mouthparts: Form, Function, Development and Performance. Springer International Publishing, Vienna, pp 127–174. https://doi.org/10.1007/978-3-030-29654-4_5

Barão KR, Ferrari A, Adami CV, Grazia J (2017) Diversity of the external thoracic scent efferent system of Carpocorini (Heteroptera: Pentatomidae) with character selection for phylogenetic inference. Zool Anz 268:102–111. https://doi.org/10.1016/j.jcz.2016.08.003

Breddin G (1903) Beiträge zur Hemipteren-fauna der Andes. Sitzungsberichte der Gesellschaft Naturforschender Freunde zu Berlin 1903:366–383.

Brozek J (2014) External Traces of Segmentation of the Labium in the Corixoidea (Hemiptera: Heteroptera: Nepomorpha). Zool Sci 31(7):445–453. https://doi.org/10.2108/zs130137

Campos LA, Grazia J (2006) Análise cladística e biogeografia de Ochlerini (Heteroptera, Pentatomidae, Discocephalinae). Iheringia, Ser Zool 96:147–163. https://doi.org/10.1590/S0073-47212006000200004

Costa Lima, AMD (1940) Capítulo XXII – Hemípteros. In: Insetos do Brasil. Tomo 2. Escola Nacional de Agronomia, pp 1–351. https://doi.org/10.5962/bhl.title.97953

Davidová-Vilímová J, Nejedlá M, Schaefer CW (2000) Dorso-abdominal scent glands and metathoracic evaporatoria in adults of central European Rhopalidae (Hemiptera: Heteroptera), with a discussion of phylogeny and higher systematics. Eur J Entomol 97(2):213–222. https://doi.org/10.14411/eje.2000.039

De Clercq P (2000) Predaceous stinkbugs (Pentatomidae: Asopinae). In: Schaefer CW, Panizzi AR (eds) Heteroptera of economic importance. CRC press, Boca Raton, pp 759–812. https://doi.org/10.1201/9781420041859

Distant WL (1911) Rhynchotal notes. — LIV. Pentatomidae from various regions. Ann Mag Nat Hist, Series 8, 7(40):338–355. https://doi.org/10.1080/00222931108692948

Goloboff PA, Morales M (2023) TNT version 1.6, with a graphical interface for MacOS and Linux, including new routines in parallel. Cladistics 39(2):144–153. https://doi.org/10.1111/cla.12524

Genevcius BC (2024) Dissecting the Pandora's box: preliminary phylogenomic insights into the internal and external relationships of stink bugs (Hemiptera: Pentatomidae). Insect Syst Divers 8(4): 10. https://doi.org/10.1093/isd/ixae024

Genevcius BC, Greve C, Koehler S, Simmons RB, Rider DA, Grazia J, Schwertner CF (2021) Phylogeny of the stink bug tribe Chlorocorini (Heteroptera, Pentatomidae) based on DNA and morphological data: the evolution of key phenotypic traits. Syst Entomol 46(2):327–338. https://doi.org/10.1111/syen.12464

Grazia J, Simões FL, Panizzi AR (2015) Morphology, ontogeny, reproduction, and feeding of true bugs. In: Panizzi AR, Grazia J (eds) True bugs (Heteroptera) of the Neotropics. Entomology in Focus, vol 2. Springer, Dordrecht, pp 21–55. https://doi.org/10.1007/978-94-017-9861-7_2

Grazia J, Panizzi AR, Greve C, Schwertner CF, Campos LA, Garbelotto TA, Fernandes JAM (2015) Stink bugs (Pentatomidae). In: Panizzi AR, Grazia J (eds) True bugs (Heteroptera) of the Neotropics. Entomology in Focus, vol 2. Springer, Dordrecht, pp 681–756. https://doi.org/10.1007/978-94-017-9861-7_22

Hischen F, Buchberger G, Plamadeala C, Armbruster O, Heiss E, Winands K, Schwarz M, Jüttler B, Heitz J, Baumgartner W (2018) The external scent efferent system of selected European true bugs (Heteroptera): a biomimetic inspiration for passive, unidirectional fluid transport. J R Soc Interface, 15(140). https://doi.org/10.1098/rsif.2017.0975

Kment P, Vilímová J (2010) Thoracic scent efferent system of Pentatomoidea (Hemiptera: Heteroptera): a review of terminology. Zootaxa 2706:1–77. https://doi.org/10.11646/zootaxa.2706.1.1

Kment P, Štys P, Vilímová J (2012) Thoracic scent efferent system and exponium of Aphylidae (Hemiptera: Heteroptera: Pentatomoidea), its architecture and function. Eur J Entomol 109(2). https://doi.org/10.14411/eje.2012.035

Kormilev NA (1949) Una especie nueva del género *Placocoris* Mayr en la Argentina (Hemiptera, Pentatomidae). Comun Inst Nac Invest Cienc Nat 1:1–12.

Kormilev NA (1951) Sobre los géneros *Vulsirea* Spinola (1837), *Ramosiana* Kormilev (1950) y *Adoxoplatys* Breddin (1903), con la descripción de tres especies nuevas. Rev Soc Entomol Arg 15:83–95.

Kormilev NA (1955) Notas sobre Pentatomoidea Neotropicales II (Hemiptera). Acta Sci Inst Invest San Miguel 1:1–16.

Kormilev NA (1956) Notas sobre Pentatomoidea Neotropicales V (Hemiptera). Acta Sci Inst Invest San Miguel 4:1–7.

Martínez, MCM (2002) Revisión genérica de la familia Cydnidae (Hemiptera-Heteroptera) en México, con un listado de las especies conocidas. An Inst Biol Ser Zool 73(2):157–192.

Mayr GL (1864) Diagnosen neuer Hemipteren. Verh Zool -Bot Ges Wien 14:903–914.

Pirán AA (1962) Hemíptera Neotrópica VI. Una nueva especie de *Zimmeria* Ruckes 1958 (Pentatomidae). Mitt. Münch. Entomol. Ges. 52:253–256.

Rider DA, Schwertner CF, Vilímová J, Rédei D, Kment P, Thomas DB (2018) Higher systematics of the Pentatomoidea. In: McPherson JE (ed) Invasive Stink Bugs and Related Species (Pentatomoidea): Biology, Higher Systematics, Semiochemistry, and Management. CRC Press, Boca Raton, pp 25–204.

Roca-Cusachs M, Schwertner CF, Kim J, Eger J, Grazia J, Jung S (2022) Opening Pandora's box: molecular phylogeny of the stink bugs (Hemiptera: Heteroptera: Pentatomidae) reveals great incongruences in the current classification. Syst Entomol 47(1):36–51. https://doi.org/10.1111/syen.12514

Roell T, Campos LA (2019) Phylogeny of Ochlerini (Hemiptera: Pentatomidae: Discocephalinae) and the evolution of the apical tarsomere in hind legs. Zool J Linn Soc 185:1137–1149. https://doi.org/10.1093/zoolinnean/zly073

Rolston LH, McDonald FJD (1979) Keys and diagnoses for the families of Western Hemisphere Pentatomoidea, subfamilies of Pentatomidae and tribes of Pentatominae (Hemiptera). J N Y Entomol Soc 87(3):189–207.

Rolston LH (1992) Key and diagnoses for the genera of Ochlerini (Hemiptera: Pentatomidae: Discocephalinae). J N Y Entomol Soc 100(1):1–41. https://biostor.org/reference/172245

Ruckes H (1958) Four new species of Neotropical pentatomids (Heteroptera, Pentatomidae). J N Y Entomol Soc 66(3/4):145–152.

Sampaio VG, Campos LA (2023) *Paropsocolis*, a new pentatomid genus with two new species from Brazil (Heteroptera, Pentatomidae, Ochlerini). Zootaxa 5323(4):553–566. https://doi.org/10.11646/zootaxa.5323.4.6

Sampaio VG, Oliveira GVD, Campos LA (2024) Revision of *Janeirona* Distant, 1911 (Hemiptera: Pentatomidae: Ochlerini) with the description of four new species from Brazil. Zootaxa 5497(4): 451–495. https://doi.org/10.11646/zootaxa.5497.4.1

Sampaio VG, Souza DCS, Rider DAR, Campos LA (in press) Revision of *Adoxoplatys* Breddin, 1903 (Hemiptera: Pentatomidae: Discocephalinae: Ochlerini) with the description of three new species from South America. Zoologia.

Schuh RT, Weirauch C (2020) True bugs of the world (Hemiptera: Heteroptera): classification and natural history. Siri Scientific Press, Rochdale.

Staddon BW (1979) The scent glands of Heteroptera. Adv Insect Physiol 14:351–418. https://doi.org/10.1016/S0065-2806(08)60055-7

Stueben M, Linsenmair KE (2008) Advances in insect preparation: bleaching, clearing and relaxing ants (Hymenoptera: Formicidae). Myrmecol News 12:15–21. https://doi.org/10.25849/myrmecol.news_012:015

Staddon BW (1986) Biology of scent glands in the Hemiptera-Heteroptera. Ann Soc entomol Fr (NS) 22:183–190. https://doi.org/10.1080/21686351.1986.12278419

Thomas DB (2021) The Moneda Bug, *Chrysodarecus moneta* Breddin = *Placocoris viridis* Mayr (Pentatomidae: Discocephalinae: Ochlerini). Zootaxa 4958(1):595–604. https://doi.org/10.11646/zootaxa.4958.1.35

Weber DC, Morrison WR III, Khrimian A, Rice KB, Leskey TC, Rodriguez-Saona C, Nielsen AL, Blaauw BR (2017) Chemical ecology of *Halyomorpha halys*: discoveries and applications. J Pest Sci 90(4):989–1008. https://doi.org/10.1007/s10340-017-0876-6

Weiler L, Barão KR, Cassis G, Grazia J (2017) Morphology of the external scent efferent system of Neotropical shield bugs (Hemiptera: Scutelleridae: Pachycorinae). Zoomorphology 136(1):29–44. https://doi.org/10.1007/s00435-016-0330-y

Weirauch C (2008) From four- to three-segmented labium in Reduviidae (Hemiptera: Heteroptera). Acta entomol Mus Natl Pragae 48(2):331–344.

TABLE AND FIGURE CAPTIONS

Table 1. Species of Pentatomidae by subfamily used in this study. ESES: external scent efferent system.

Fig. 1 Dorsal habitus of the studied species. **a** *Adoxoplatys comis* Breddin, 1903; **b** *Adoxoplatys brasiliensis* Kormilev, 1951; **c** *Adoxoplatys gallardoi* Kormilev, 1951; **d** *Neoadoxoplatys longirostra* Ruckes, 1958; **e** *Janeirona insignis* Distant, 1911; **f** *Janeirona bergi* (Kormilev, 1956); **g** *Janeirona costalimai* (Pirán, 1962); **h** *Janeirona flavipes* Sampaio and Campos, 2024; i *Janeirona stenosa* Sampaio and Campos, 2024; **j** *Paropsocolis convergens* Sampaio and Campos, 2023; **k** *Placocoris viridis* Mayr, 1864; **l** *Macropygium reticulare* (Fabricius, 1803); **m** *Edessa rufomarginata* (De Geer, 1773); **n** *Euschistus heros* (Fabricius, 1798); **o** *Chinavia obstinata* (Stål, 1860). Scale bars = 5 mm.

Fig. 2 Labium of *Adoxoplatys brasiliensis* Kormilev, 1951, with the detail of intercalary segment. Scale bars: **a** = 1 mm, **b** = 100 µm.

Fig. 3 Longitudinal section of intercalary segment of *Adoxoplatys comis* Breddin, 1903. Arrows indicates apodemes. Scale bars: **a** = 200 µm, **b** = 50 µm, **c** = 50 µm.

Fig. 4 Comparison of intercalary segments of **a** *Adoxoplatys comis* Breddin, 1903; **b** *Adoxoplatys brasiliensis* Kormilev, 1951; **c** *Adoxoplatys gallardoi* Kormilev, 1951; **d** *Neoadoxoplatys longirostra* Ruckes, 1958. Scale bars = 100 µm.

Fig. 5 Comparison of intercalary segments of **a** *Janeirona insignis* Distant, 1911; **b** *Janeirona bergi* (Kormilev, 1956); **c** *Janeirona costalimai* (Pirán, 1962); **d** *Janeirona flavipes* Sampaio and Campos, 2024; **e** *Paropsocolis convergens* Sampaio and Campos, 2023. Scale bars = 100 µm.

Fig. 6 Comparison of intercalary segments of **a** *Placocoris viridis* Mayr, 1864; **b** *Macropygium reticulare* (Fabricius, 1803); **c** *Edessa rufomarginata* (De Geer, 1773); **d** *Euschistus heros* (Fabricius, 1798); **e** *Chinavia obstinata* (Stål, 1860). Scale bars = 100 µm.

Fig. 7 External scent efferent system map over the meso- and metapleuron of *Janeirona insignis* Distant, 1911. Abbreviations: mf = peritremal median furrow; mse = mesopleural evaporatorium (blue shaded); mte = metapleural evaporatorium (green shaded); o = ostiole; op = ostiolar plate (dashed line); p = peritreme (orange shaded); s = spiracular filter system (pink shaded). Scale bar = 500 µm.

Fig. 8 External scent efferent system of *Adoxoplatys comis* Breddin, 1903. **a** meso- and metapleuron; **b** peritreme; **c** peritremal surface; **d** detail of evaporatorium; **e** spiracular filter system. Scale bars: **a** = 500 µm, **b** = 100 µm, **c**, **d** = 10 µm, **e** = 20 µm.

Fig. 9 External scent efferent system of *Adoxoplatys brasiliensis* Kormilev, 1951. **a** meso- and metapleuron; **b** peritreme; **c** peritremal surface; **d** detail of evaporatorium; **e** spiracular filter system. Scale bars: **a** = 500 µm, **b** = 100 µm, **c**–**e** = 10 µm.

Fig. 10 External scent efferent system of *Janeirona insignis* Distant, 1911. **a** meso- and metapleuron; **b** peritreme; **c** peritremal surface; **d** detail of evaporatorium; **e** spiracular filter system. Scale bars: **a** = 500 µm, **b** = 300 µm, **c**, **d** = 10 µm, **e** = 20 µm.

Fig. 11 External scent efferent system of *Janeirona bergi* (Kormilev, 1956). **a** meso- and metapleuron; **b** peritreme; **c** peritremal surface; **d** detail of evaporatorium; **e** spiracular filter system. Scale bars: **a** = 500 µm, **b** = 300 µm, **c**, **b** = 10 µm, **e** = 20 µm.

Fig. 12 External scent efferent system of *Janeirona stenosa* Sampaio and Campos, 2024. **a** meso- and metapleuron; **b** peritreme; **c** peritremal surface; **d** detail of evaporatorium; **e** spiracular filter system. Scale bars: **a** = 500 µm, **b** = 300 µm, **c, d** = 10 µm, **e** = 20 µm.

Fig. 13 External scent efferent system of *Paropsocolis convergens* Sampaio and Campos, 2023. **a** meso- and metapleuron; **b** peritreme; **c** peritremal surface; **d** detail of evaporatorium; **e** spiracular filter system. Scale bars: **a** = 500 µm, **b** = 300 µm, **c, d** = 10 µm, **e** = 30 µm.

Fig. 14 External scent efferent system of *Placocoris viridis* Mayr, 1864. **a** meso- and metapleuron; **b** peritreme; **c** peritremal surface; **e** detail of evaporatoriu; **e** spiracular filter system. Scale bars: **a** = 500 µm, **b** = 100 µm, **c-e** = 10 µm.

Fig. 15 External scent efferent system of *Macropygium reticulare* (Fabricius, 1803). **a** meso- and metapleuron; **b** peritreme; **c** peritremal surface; **d** detail of evaporatoriu; **e** spiracular filter system. Scale bars: **a** = 1 mm, **b** = 200 µm, **c-e** = 10 µm.

Fig. 16 External scent efferent system of *Edessa rufomarginata* (De Geer, 1773). **a** meso- and metapleuron, **b** peritreme; **c** peritremal surface; **d** detail of evaporatorium; **e** spiracular filter system. Scale bars: **a** = 1 mm, **b** = 200 µm, **c-e** = 10 µm.

Fig. 17 External scent efferent system of *Euschistus heros* (Fabricius, 1798). **a** meso- and metapleuron; **b** peritreme; **c** peritremal surface; **d** detail of evaporatorium; **e** spiracular filter system. Scale bars: **a** = 500 µm, **b** = 100 µm, **c**, **d** = 10 µm, **e** = 20 µm.

Fig. 18 External scent efferent system of *Chinavia obstinata* (Stål, 1860). **a** meso- and metapleuron; **b** peritreme; **c** peritremal surface; **d** detail of evaporatorium; **e** spiracular filter system. Scale bars: **a** = 1 mm, **b** = 100 µm, **c**, **d** = 10 µm, **e** = 20 µm.